Fermion mass hierarchies from vector-like families with an extended 2HDM and a possible explanation for the electron and muon anomalous magnetic moments

Huchan Lee

University of Southampton, Physics and Astronomy

31st May, 2021

1. Introduction

There are long-established anomalies which are not addressed by the SM such as muon and electron anomalous magnetic moments.

$$\Delta a_\mu = a_\mu^{\text{Exp}} - a_\mu^{\text{SM}} = (26.1 \pm 8.0) \times 10^{-10}, \qquad \Delta a_e = a_e^{\text{Exp}} - a_e^{\text{SM}} = (-0.88 \pm 0.36) \times 10^{-12} \tag{1}$$

When trying to explain both anomalies at 1σ constraint, a main difficulty arises from the sign of each anomaly.

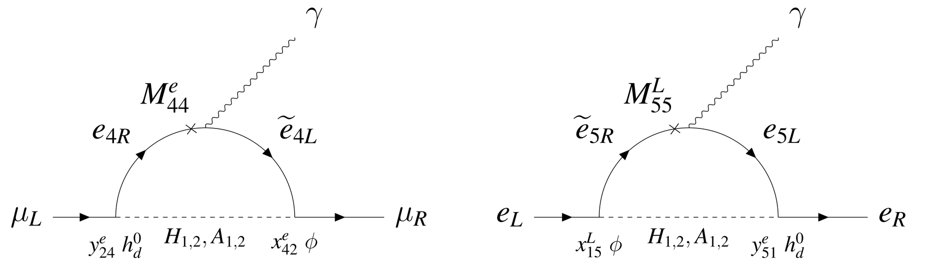

Figure 1: Diagrams contributing to muon anomalous magnetic moment(left) and electron anomalous magnetic moment(right) where $H_{1,2}$ are CP-even non-SM scalars and $A_{1,2}$ are CP-odd scalars in the physical basis

Reminding the sign of each anomaly at each sigma, it is

$$\Delta a_\mu = +, \quad \Delta a_e = - \quad \text{at 1 and } 2\sigma \qquad \Delta a_\mu = +, \quad \Delta a_e = + \quad \text{at } 3\sigma \tag{2}$$

The Higgs mechanism provides a nice explanation on fermion's mass, however, it does not tell why one mass is relatively big or small.

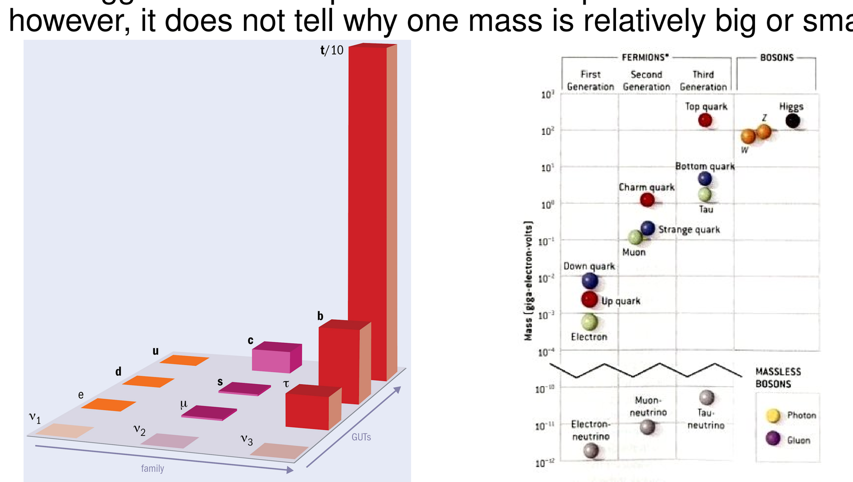

Figure 2: Hierarchical structure of the SM

The described phenomenology can be tackled by inclusion of vector-like (VL) families.

- Muon and electron $g-2$
- Hierarchy of the SM

} vector-like families

One vector-like family can get second and third SM generations massive, while the first remains massless[1]. We also enlarge the gauge symmetry with the global $U(1)'$ symmetry.

- The local $U(1)'$ symmetry features Z' boson
- The global $U(1)'$ symmetry does not have the one but allows one more non-SM scalar.

Within this BSM model frame, we focus on

- the W boson exchange at one-loop level to explain $\Delta a_{\mu,e}$, while being consistent on $\mu \to e\gamma$ constraint.
- We next focus on the scalar exchange at one-loop level in the case where no charged lepton mixing arises.

2. The origin of SM Yukawa couplings from VL families

We assume that the SM Yukawa Lagrangian is the low energy limit of an extended theory with enlarged symmetry and particle spectrum

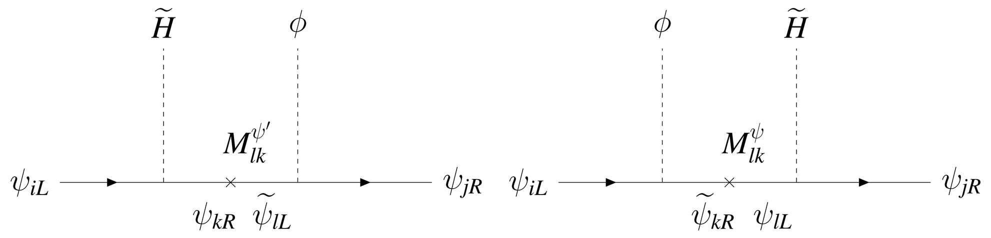

Figure 3: Diagrams in the model which lead to the effective Yukawa interactions, where $\psi, \psi' = Q, u, d, L, e$(neutrinos will be treated separately) $i,j = 1,2,3$, $k,l = 4,5$, M_{lk} is vector-like mass and $\widetilde{H} = i\sigma_2 H^*, H = H_{u,d}$

The diagrams of Figure 3 lead to the effective SM Yukawa interactions.

$$\mathcal{L}_{\text{eff}}^{\text{Yukawa}} = \frac{x_{lj}^{\psi'}\langle\phi\rangle}{M_{lk}^{\psi'}} y_{ik}^{\psi}\overline{\psi}_{iL}\widetilde{H}\psi_{jR} + \frac{x_{ik}^{\psi}\langle\phi\rangle}{M_{lk}^{\psi}} y_{lj}^{\psi}\overline{\psi}_{iL}\widetilde{H}\psi_{jR} + \text{h.c.} \tag{3}$$

Our BSM model takes the form as follows:

Field	Q_{iL}	u_{iR}	d_{iR}	L_{iL}	e_{iR}	Q_{kL}	u_{kR}	d_{kR}	L_{kL}	e_{kR}	ν_{kR}	$\widetilde{Q}_{kR}$	$\widetilde{u}_{kL}$	$\widetilde{d}_{kL}$	$\widetilde{L}_{kR}$	$\widetilde{e}_{kL}$	$\widetilde{\nu}_{kR}$	ϕ	H_u	H_d
$\mathrm{SU(3)_C}$	**3**	**3**	**3**	**1**	**1**	**3**	**3**	**3**	**1**	**1**	**1**	**3**	**3**	**3**	**1**	**1**	**1**	**1**	**1**	**1**
$\mathrm{SU(2)_L}$	**2**	**1**	**1**	**2**	**1**	**2**	**1**	**1**	**2**	**1**	**1**	**2**	**1**	**1**	**2**	**1**	**1**	**1**	**2**	**2**
$\mathrm{U(1)_Y}$	$\frac{1}{6}$	$\frac{2}{3}$	$-\frac{1}{3}$	$-\frac{1}{2}$	1	$\frac{1}{6}$	$\frac{2}{3}$	$-\frac{1}{3}$	$-\frac{1}{2}$	-1	0	$\frac{1}{6}$	$\frac{2}{3}$	$-\frac{1}{3}$	$-\frac{1}{2}$	-1	0	0	$\frac{1}{2}$	$-\frac{1}{2}$
$\mathrm{U(1)'}$	0	0	0	0	0	1	−1	−1	1	−1	−1	1	−1	−1	1	−1	−1	1	−1	−1

Table 1: An extended 2HDM with two vector-like (VL) families plus global $U(1)'$ symmetry where $i,j = 1,2,3$ and $k,l = 4,5$

1. The SM particles are neutral under the $U(1)'$ symmetry to keep the SM Yukawa interactions from arising.
2. Once the flavon ϕ develops its vev, the effective SM Yukawa interactions get to have a proportional factor $\langle\phi\rangle/M$.

The possible diagrams contributing to the low energy quark Yukawa interaction are given in Figure 4:

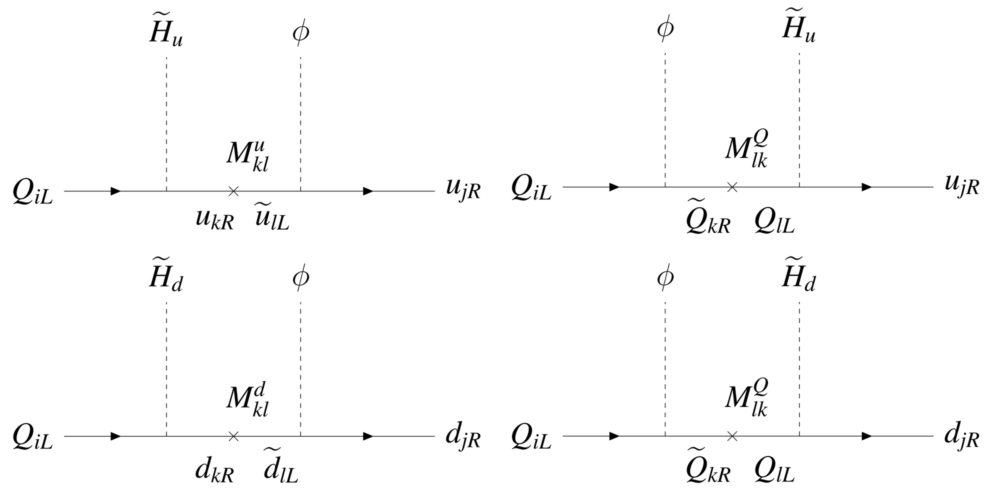

Figure 4: Diagrams in the model which lead to the effective Yukawa interactions for the up quark sector(two above diagrams) and the down quark sector(two below diagrams) in mass insertion approximation, where $i,j = 1,2,3$ and $k,l = 4,5$ and M_{lk} is vector-like mass.

The possible diagrams giving rise to the charged lepton Yukawa interactions are shown in the below Figure:

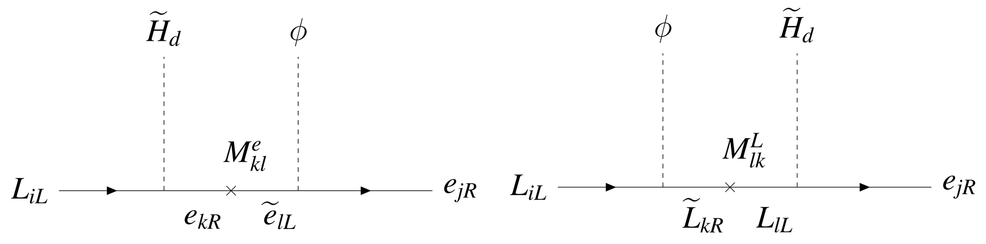

Figure 5: Diagrams in the model which lead to the effective Yukawa interactions for the charged lepton sector

The corresponding diagram for the neutrino sector in the mass insertion approximation reads:

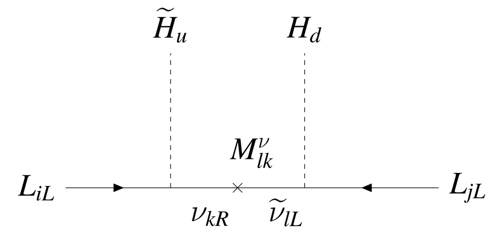

Figure 6: Type 1b seesaw mechanism

3. Effective Yukawa matrices using a mixing formalism

Consider a 7×7 mass matrix for Dirac fermions:

$$M^{\psi} = \begin{array}{c|ccccccc} & \psi_{1R} & \psi_{2R} & \psi_{3R} & \psi_{4R} & \psi_{5R} & \widetilde{\psi}_{4R} & \widetilde{\psi}_{5R} \\ \hline \overline{\psi}_{1L} & 0 & 0 & 0 & y_{14}^{\psi}\langle\widetilde{H}^0\rangle & y_{15}^{\psi}\langle\widetilde{H}^0\rangle & x_{14}^{\psi}\langle\phi\rangle & x_{15}^{\psi}\langle\phi\rangle \\ \overline{\psi}_{2L} & 0 & 0 & 0 & y_{24}^{\psi}\langle\widetilde{H}^0\rangle & y_{25}^{\psi}\langle\widetilde{H}^0\rangle & x_{24}^{\psi}\langle\phi\rangle & x_{25}^{\psi}\langle\phi\rangle \\ \overline{\psi}_{3L} & 0 & 0 & 0 & y_{34}^{\psi}\langle\widetilde{H}^0\rangle & y_{35}^{\psi}\langle\widetilde{H}^0\rangle & x_{34}^{\psi}\langle\phi\rangle & x_{35}^{\psi}\langle\phi\rangle \\ \overline{\psi}_{4L} & y_{41}^{\psi}\langle\widetilde{H}^0\rangle & y_{42}^{\psi}\langle\widetilde{H}^0\rangle & y_{43}^{\psi}\langle\widetilde{H}^0\rangle & 0 & 0 & M_{44}^{\psi} & M_{45}^{\psi} \\ \overline{\psi}_{5L} & y_{51}^{\psi}\langle\widetilde{H}^0\rangle & y_{52}^{\psi}\langle\widetilde{H}^0\rangle & y_{53}^{\psi}\langle\widetilde{H}^0\rangle & 0 & 0 & M_{54}^{\psi} & M_{55}^{\psi} \\ \overline{\widetilde{\psi}}_{4L} & x_{41}^{\psi'}\langle\phi\rangle & x_{42}^{\psi'}\langle\phi\rangle & x_{43}^{\psi'}\langle\phi\rangle & M_{44}^{\psi'} & M_{45}^{\psi'} & 0 & 0 \\ \overline{\widetilde{\psi}}_{5L} & x_{51}^{\psi'}\langle\phi\rangle & x_{52}^{\psi'}\langle\phi\rangle & x_{53}^{\psi'}\langle\phi\rangle & M_{54}^{\psi'} & M_{55}^{\psi'} & 0 & 0 \end{array}, \tag{4}$$

After vanishing v_ϕ terms by rotating them, we can read off the upper 3×3 mass matrix for SM charged leptons.

$$y_{ij}^e = \begin{pmatrix} s_{15}^L y_{51}^e + y_{15}^e\theta_{15}^e & s_{15}^L y_{52}^e + y_{15}^e\theta_{25}^e & s_{15}^L y_{53}^e + y_{15}^e\theta_{35}^e \\ s_{25}^L y_{51}^e + y_{25}^e\theta_{15}^e & s_{25}^L y_{52}^e + y_{24}^e\theta_{24}^e + y_{25}^e\theta_{25}^e & s_{25}^L y_{53}^e + y_{24}^e\theta_{34}^e + y_{25}^e\theta_{35}^e \\ s_{35}^L y_{51}^e + y_{35}^e\theta_{15}^e & s_{35}^L y_{52}^e + y_{34}^e\theta_{24}^e + y_{35}^e\theta_{25}^e & s_{34}^L y_{43}^e + s_{35}^L y_{53}^e + y_{34}^e\theta_{34}^e + y_{35}^e\theta_{35}^e \end{pmatrix} \tag{5}$$

4. Analytic arguments for $\Delta a_{\mu,e}$ and $\mathrm{BR}(\mu \to e\gamma)$ with W boson

The simplified mass matrix for neutrinos in our model is given by:

$$M^{\nu} \approx \begin{array}{c|ccc|cc} & \nu_{1L} & \nu_{2L} & \nu_{3L} & \overline{\nu}_{4R} & \widetilde{\nu}_{4R} \\ \hline \nu_{1L} & 0 & 0 & 0 & y_1^{\nu}v_u & \epsilon y_1^{\nu\prime}v_d \\ \nu_{2L} & 0 & 0 & 0 & y_2^{\nu}v_u & \epsilon y_2^{\nu\prime}v_d \\ \nu_{3L} & 0 & 0 & 0 & y_3^{\nu}v_u & \epsilon y_3^{\nu\prime}v_d \\ \hline \overline{\nu}_{4R} & y_1^{\nu}v_u & y_2^{\nu}v_u & y_3^{\nu}v_u & 0 & M_{44}^{\nu} \\ \widetilde{\nu}_{4R} & \epsilon y_1^{\nu\prime}v_d & \epsilon y_2^{\nu\prime}v_d & \epsilon y_3^{\nu\prime}v_d & M_{44}^{\nu} & 0 \end{array} \equiv \begin{pmatrix} 0 & m_D \\ m_D^T & M_N \end{pmatrix}, \tag{6}$$

where $v_u(v_d)$ is the vev of $\widetilde{H}_u(H_d)$, v_u runs from $246/\sqrt{2}\,\mathrm{GeV} \simeq 174\,\mathrm{GeV}$ to $246\,\mathrm{GeV}$ and $v_u^2 + v_d^2 = (246\,\mathrm{GeV})^2$. The next step is to read off Weinberg operator for neutrinos from the neutrino mass matrix.

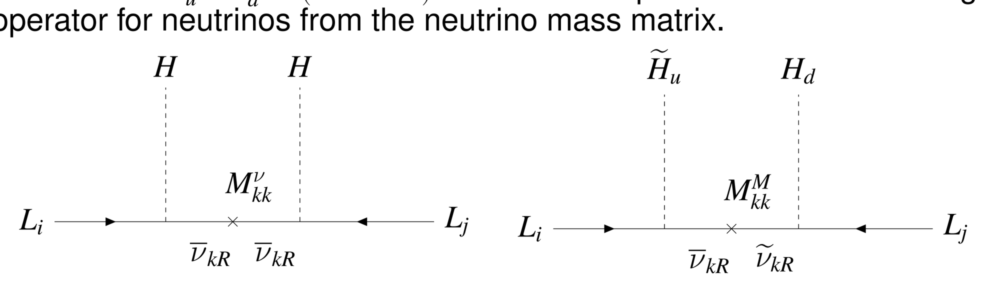

Figure 7: The conventional Weinberg operator (or type 1a seesaw mechanism; left) and a Weinberg-like operator (or type 1b seesaw mechanism; right)

Here, we can read off nature of vector-like mass by looking at the renormalizable Lagrangian.

$$\mathcal{L}_{\nu}^{\text{Yukawa+Mass}} = y_i^{\nu}\overline{L}_{iL}\widetilde{H}_u\nu_{kR} + \epsilon y_i^{\nu\prime}\overline{L}_{iL}H_d\widetilde{\overline{\nu}}_{kR} + M_{kk}^{\nu}\widetilde{\overline{\nu}}_{kR}\nu_{kR} + \text{h.c.}, \tag{7}$$

The neutrino mass matrix of Equation 6 can be diagonalized by the unitary mixing matrix U:

$$U^T \begin{pmatrix} 0 & m_D^T \\ m_D & M_N \end{pmatrix} U = \begin{pmatrix} m_\nu^{\text{diag}} & 0 \\ 0 & M_N^{\text{diag}} \end{pmatrix}, \tag{8}$$

The unitary mixing matrix U is defined by multiplication of two unitary matrices which we call U_A and U_B, respectively:

$$U = U_A \cdot U_B$$
$$U_A = \exp\begin{pmatrix} 0 & \Theta \\ -\Theta^\dagger & 0 \end{pmatrix} \simeq \begin{pmatrix} I - \frac{\Theta\Theta^\dagger}{2} & \Theta \\ -\Theta^\dagger & I - \frac{\Theta\Theta^\dagger}{2} \end{pmatrix} \quad \text{at leading order in } \Theta \tag{9}$$
$$U_B = \begin{pmatrix} U_{\text{PMNS}} & 0 \\ 0 & I \end{pmatrix}$$

where $\Theta\Theta^\dagger/2$ is known as the deviation of unitarity η, which consists of VL mass M_{44}^{ν} and the Yukawa couplings $y_{i,j}^{\nu}$

$$\eta_{ij} = \frac{\Theta_i\Theta_j^\dagger}{2} = \frac{1}{2}\frac{m_D^\dagger m_D}{M_N^2} = \frac{1}{2M_{44}^{\nu 2}}\left(v_u^2 y_i^{\nu*}y_j^{\nu} + \epsilon^2 v_d^2 y_i^{\nu\prime*}y_j^{\nu\prime}\right) \simeq \frac{v_u^2}{2M_{44}^{\nu 2}}y_i^{\nu*}y_j^{\nu}. \tag{10}$$

Consider the three light neutrinos in SM for the CLFV $\mu \to e\gamma$ first.

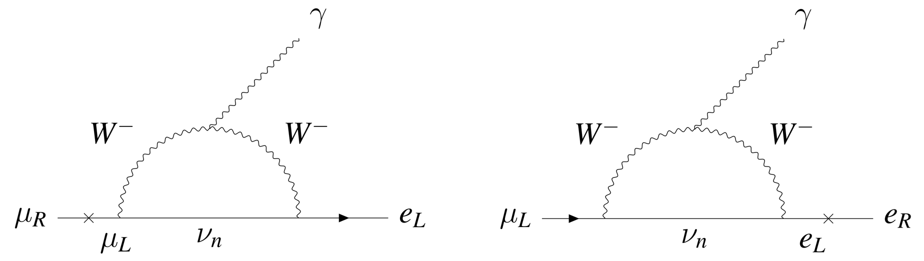

Figure 8: Diagrams for CLFV $\mu \to e\gamma$ decay with all SM neutrinos($n = 1,2,3$)

The SM prediction with neutrinos gives a very suppressed sensitivity [2]

$$\mathrm{BR}(\mu \to e\gamma) = 10^{-55} \quad (\text{with } \nu_{1,2,3}). \tag{11}$$

This impractical sensitivity can be enhanced to the observable level by introducing heavy vector-like neutrinos.

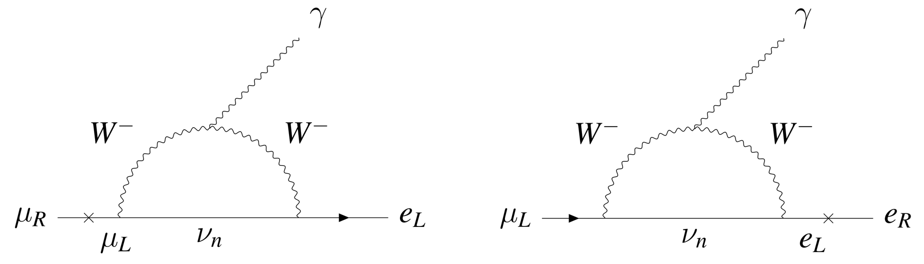

Figure 9: Diagrams for CLFV $\mu \to e\gamma$ decay with all neutrinos($n = 1,2,3,4,5$)

The final form for $\mu \to e\gamma$ decay with all neutrinos in this model reads:

$$\mathrm{BR}(\mu \to e\gamma) = \frac{3\alpha_{\text{em}}}{8\pi}|\eta_{21}|^2\left(F(x_4) - F(0)\right)^2, \tag{12}$$

where F is a loop function given by ($x_n = M_n^2/M_W^2$)

$$F(x_n) = \frac{10 - 43x_n + 78x_n^2 - (49 - 18\log x_n)x_n^3 + 4x_n^4}{3(x_n - 1)^4}. \tag{13}$$

We derive our prediction for the muon anomalous magnetic moment in this section. Consider two possible diagrams for muon(electron) anomalous magnetic moment at one-loop level in Figure 10

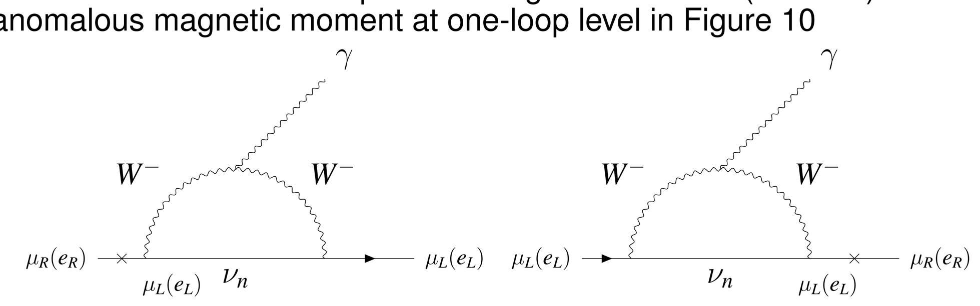

Figure 10: Diagrams for muon anomalous magnetic moment with all neutrinos($n = 1,2,3,4,5$)

Our prediction for muon(electron) anomalous magnetic moment at one-loop level is

$$\Delta a_\mu = \frac{\alpha_W}{16\pi}\frac{m_\mu^2}{M_W^2}\eta_{22}\left(F(x_4) - F(0)\right), \qquad \Delta a_e = \frac{\alpha_W}{16\pi}\frac{m_e^2}{M_W^2}\eta_{11}\left(F(x_4) - F(0)\right). \tag{14}$$

As for the constraint of deviation of unitarity η with the CLFV $\mu \to e\gamma$ decay at 1σ, it is given by[3, 4]

$$|\eta_{21}| \leq 8.4 \times 10^{-6}. \tag{15}$$

As in the constraint for η_{21} in Equation 15, the other non-unitarities $\eta_{11,22}$ for electron and muon anomalous mangetic moment are given by[5]

$$\eta_{11} < 4.2 \times 10^{-4} \text{ (for NH)}, \quad < 4.8 \times 10^{-4} \text{ (for IH)} \qquad \eta_{22} < 2.9 \times 10^{-7} \text{ (for NH)}, \quad < 2.4 \times 10^{-7} \text{ (for IH)} \tag{16}$$

Then we are ready to calculate impact of muon and electron $g-2$ with the given bound of Equation 16.

$$\Delta a_\mu = \frac{\alpha_W}{16\pi}\frac{m_\mu^2}{M_W^2}\eta_{22}\left(F(x_4) - F(0)\right) \simeq -6.6(-5.5) \times 10^{-16} \qquad \Delta a_e = \frac{\alpha_W}{16\pi}\frac{m_e^2}{M_W^2}\eta_{11}\left(F(x_4) - F(0)\right) \simeq -2.2(-2.6) \times 10^{-17} \tag{17}$$

5. Analytic arguments for $\Delta a_{\mu,e}$ and $\mathrm{BR}(\mu \to e\gamma)$ with scalars

The relevant sector for muon and electron $g-2$ with scalar exchange is charged lepton, so revisit the effective Yukawa matrix for the charged leptons.

$$y_{ij}^e = \begin{pmatrix} 0 & 0 & 0 \\ 0 & y_{24}^e x_{42}^e & y_{24}^e x_{43}^e \\ 0 & y_{34}^e x_{42}^e & y_{34}^e x_{43}^e \end{pmatrix}\frac{\langle\phi\rangle}{M_{44}^e} + \begin{pmatrix} y_{15}^e x_{51}^e & y_{15}^e x_{52}^e & y_{15}^e x_{53}^e \\ y_{25}^e x_{51}^e & y_{25}^e x_{52}^e & y_{25}^e x_{53}^e \\ y_{35}^e x_{51}^e & y_{35}^e x_{52}^e & y_{35}^e x_{53}^e \end{pmatrix}\frac{\langle\phi\rangle}{M_{55}^e} + \begin{pmatrix} y_{51}^e x_{15}^L & y_{52}^e x_{15}^L & y_{53}^e x_{15}^L \\ y_{51}^e x_{25}^L & y_{52}^e x_{25}^L & y_{53}^e x_{25}^L \\ y_{51}^e x_{35}^L & y_{52}^e x_{35}^L & y_{53}^e x_{35}^L \end{pmatrix}\frac{\langle\phi\rangle}{M_{55}^L} + \begin{pmatrix} 0 & 0 & 0 \\ 0 & 0 & 0 \\ 0 & 0 & x_{34}^L y_{43}^e \end{pmatrix}\frac{\langle\phi\rangle}{M_{44}^L}. \tag{18}$$

The only diagonal components should alive in the mass matrix. In order to make the mass matrix diagonal, we assume that $y_{34}^e = x_{43}^e = y_{15,25,35}^e = x_{51,52,53}^e = x_{25,35}^L = y_{52,53}^e = 0$. Then, the mass matrix is reduced to

$$y_{ij}^e = \begin{pmatrix} y_{51}^e s_{15}^L & 0 & 0 \\ 0 & y_{24}^e s_{24}^e & 0 \\ 0 & 0 & y_{43}^e s_{34}^L \end{pmatrix}, \tag{19}$$

where $s_{15}^L \simeq x_{15}^L\langle\phi\rangle/M_{55}^L$, $s_{24}^e \simeq x_{42}^e\langle\phi\rangle/M_{44}^e$, $s_{34}^L \simeq x_{34}^L\langle\phi\rangle/M_{44}^L$ and the diagonal elements from top-left to bottom-right should be responsible for electron, muon and tau Yukawa constants, respectively. The charged lepton mass matrix with the assumption is:

$$M^e = \begin{array}{c|cccc} & e_{1R} & e_{2R} & e_{4R} & \widetilde{L}_{5R} \\ \hline \overline{L}_{1L} & 0 & 0 & 0 & x_{15}^L v_\phi \\ \overline{L}_{2L} & 0 & 0 & y_{24}^e v_d & 0 \\ \overline{L}_{5L} & y_{51}^e v_d & 0 & 0 & M_{55}^L \\ \overline{\widetilde{e}}_{4L} & 0 & x_{42}^e v_\phi & M_{44}^e & 0 \end{array}. \tag{20}$$

The reduced charged lepton mass matrix in Equation 20 clearly tells that no mixing between charged leptons arise so the branching ratio of $\mu \to e\gamma$ is naturally satisfied under this scenario. The scalar exchange for both anomalies can be realized by closing the Higgs sectors in Figure 5 as per Figure 11.

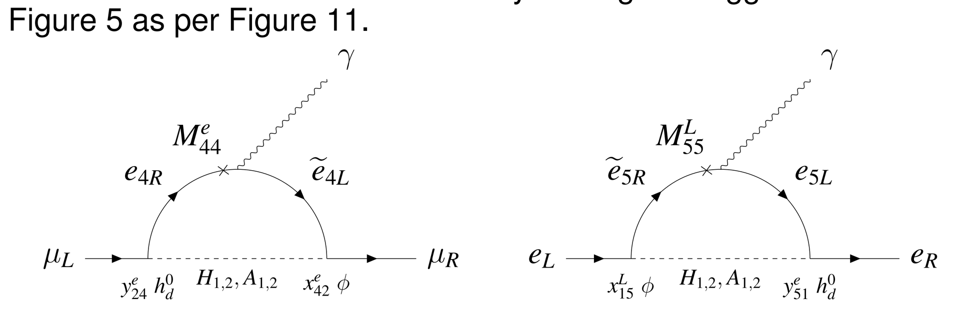

Figure 11: Diagrams contributing to muon anomalous magnetic moment(left) and electron anomalous magnetic moment(right) where $H_{1,2}$ are CP-even non-SM scalars and $A_{1,2}$ are CP-odd scalars in the physical basis

The scalar potential of the model under consideation takes the form:

$$\begin{aligned} V =& \mu_1^2\left(H_u H_u^\dagger\right) + \mu_2^2\left(H_d H_d^\dagger\right) + \mu_3^2(\phi\phi^*) - \mu_{\text{sb}}^2\left[\phi^2 + (\phi^*)^2\right] + \lambda_1\left(H_u H_u^\dagger\right)^2 + \lambda_2\left(H_d H_d^\dagger\right)^2 \\ &+ \lambda_3\left(H_u H_u^\dagger\right)\left(H_d H_d^\dagger\right) + \lambda_4\left(H_u H_d^\dagger\right)\left(H_d H_u^\dagger\right) + \lambda_5\left(\varepsilon_{ij}H_u^i H_d^j\phi^2 + h.c\right) \\ &+ \lambda_6(\phi\phi^*)^2 + \lambda_7(\phi\phi^*)\left(H_u H_u^\dagger\right) + \lambda_8(\phi\phi^*)\left(H_d H_d^\dagger\right), \end{aligned} \tag{21}$$

where

1. $\lambda_i (i = 1,2,\cdots,8)$: dimensionless parameters, $\mu_j (j = 1,2,3)$: dimensionful parameters
2. We consider the $U(1)'$ symmetry as global in this model to avoid Z' constraint.

$$H_u = \begin{pmatrix} H_u^+ \\ v_u + \frac{1}{\sqrt{2}}\left(\mathrm{Re}\,H_u^0 + i\,\mathrm{Im}\,H_u^0\right) \end{pmatrix}, \quad H_d = \begin{pmatrix} v_d + \frac{1}{\sqrt{2}}\left(\mathrm{Re}\,H_d^0 + i\,\mathrm{Im}\,H_d^0\right) \\ H_d^- \end{pmatrix}, \quad \phi = \frac{1}{\sqrt{2}}\left(v_\phi + \mathrm{Re}\,\phi + i\,\mathrm{Im}\,\phi\right). \tag{22}$$

$$\begin{aligned} \mu_1^2 &= -2\lambda_1 v_1^2 - \lambda_3 v_2^2 - \frac{1}{2}\lambda_7 v_3^2 - \frac{\lambda_5 v_2 v_3^2}{2v_1}, \\ \mu_2^2 &= -\lambda_3 v_1^2 - \frac{\lambda_5 v_3^2 v_1}{2v_2} - 2\lambda_2 v_2^2 - \frac{1}{2}\lambda_8 v_3^2, \\ \mu_3^2 &= -\lambda_8 v_2^2 - \lambda_6 v_3^2 - v_1\left(2\lambda_5 v_2 + \lambda_7 v_1\right) - 2\mu_{\text{sb}}^2. \end{aligned} \tag{23}$$

The rate for the $h \to \gamma\gamma$ decay is given by:

$$\Gamma(h \to \gamma\gamma) = \frac{\alpha_{\text{em}}^2 m_h^3}{256\pi^3 v^2}\left|\sum_f a_{hff}N_C Q_f^2 F_{1/2}(\rho_f) + a_{hWW}F_1(\rho_W) + \frac{C_{hH^\pm H^\mp}v}{2m_{H^\pm}^2}F_0(\rho_{H_k^\pm})\right|^2, \tag{24}$$

where ρ_i are the mass ratios $\rho_i = \frac{m_h^2}{4M_i^2}$ with $M_i = m_f, M_W$; α_{em} is the fine structure constant; N_C is the color factor ($N_C = 1$ for leptons and $N_C = 3$ for quarks) and Q_f is the electric charge of the fermion in the loop. The necessary deviation factors for our numerical analysis are:

$$a_{htt} \simeq 1, \quad a_{hWW} = \frac{v_1}{\sqrt{v_1^2 + v_2^2}} \tag{25}$$

The Lagrangian for the muon anomalous magnetic moment is:

$$\begin{aligned} \mathcal{L}_{\Delta a_\mu} =& y_{24}^e\mu\left((R_e^T)_{22}H_1 + (R_e^T)_{23}H_2 - i\gamma^5(R_o^T)_{22}A_1 - i\gamma^5(R_o^T)_{23}A_2\right)\overline{e}_4 \\ &+ x_{42}^e\widetilde{e}_4\left((R_e^T)_{32}H_1 + (R_e^T)_{33}H_2 - i\gamma^5(R_o^T)_{32}A_1 - i\gamma^5(R_o^T)_{33}A_2\right)\overline{e}_2 + M_{44}^e\widetilde{e}_4\overline{e}_4 + \text{h.c.} \end{aligned} \tag{26}$$

Then, it follows that the muon and electron anomalous magnetic moments in the scenario of diagonal SM charged lepton mass matrix takes the form:

$$\begin{aligned} \Delta a_\mu = y_{24}^e x_{42}^e\frac{m_\mu^2}{8\pi^2}\Big[&\left(R_e^T\right)_{22}\left(R_e^T\right)_{32}I_S^{(\mu)}(m_{e_4}, m_{H_1}) + \left(R_e^T\right)_{23}\left(R_e^T\right)_{33}I_S^{(\mu)}(m_{e_4}, m_{H_2}) \\ &- \left(R_o^T\right)_{22}\left(R_o^T\right)_{32}I_P^{(\mu)}(m_{e_4}, m_{A_1}) - \left(R_o^T\right)_{23}\left(R_o^T\right)_{33}I_P^{(\mu)}(m_{e_4}, m_{A_2})\Big] \\ \Delta a_e = y_{51}^e x_{15}^L\frac{m_e^2}{8\pi^2}\Big[&\left(R_e^T\right)_{22}\left(R_e^T\right)_{32}I_S^{(e)}(m_{e_5}, m_{H_1}) + \left(R_e^T\right)_{23}\left(R_e^T\right)_{33}I_S^{(e)}(m_{e_5}, m_{H_2}) \\ &- \left(R_o^T\right)_{22}\left(R_o^T\right)_{32}I_P^{(e)}(m_{e_5}, m_{A_1}) - \left(R_o^T\right)_{23}\left(R_e^T\right)_{33}I_P^{(E)}(m_{e_5}, m_{A_2})\Big], \end{aligned} \tag{27}$$

where the loop integrals are given by:

$$I_{S(P)}^{(e,\mu)}(m_E, m_S) = \int_0^1 \frac{x^2\left(1 - x \pm \frac{m_E}{m_{e,\mu}}\right)}{m_\mu^2 x^2 + \left(m_E^2 - m_{e,\mu}^2\right)x + m_{S,P}^2(1 - x)}dx \tag{28}$$

and $S(P)$ means scalar(pseudo scalar) and E means vector-like family.

6. Numerical analysis of the scalar exchange

To begin with, we consider the parameter spaces for the muon anomaly versus electron anomaly with a mass parameter which attends both anomalies ($H_{1,2}, A_{1,2}$) and does not ($H^\pm$) in Figure 12.

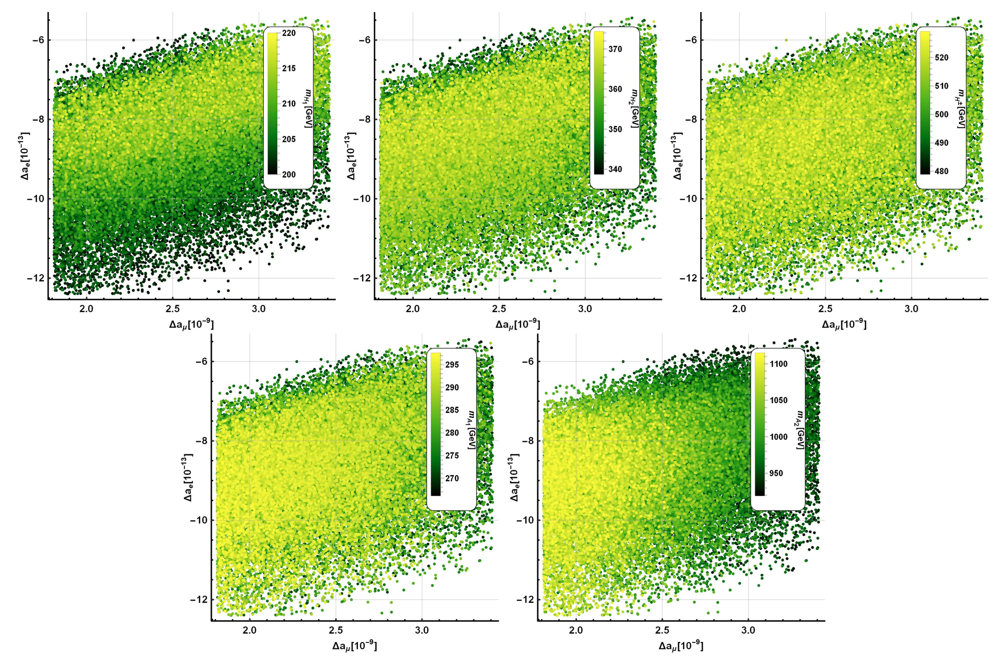

Figure 12: Available parameter spaces for the muon anomaly versus electron anomaly with a mass parameter

We investigate a correlation for an anomaly versus a relevant mass parameter with another anomaly in bar in Figure 13.

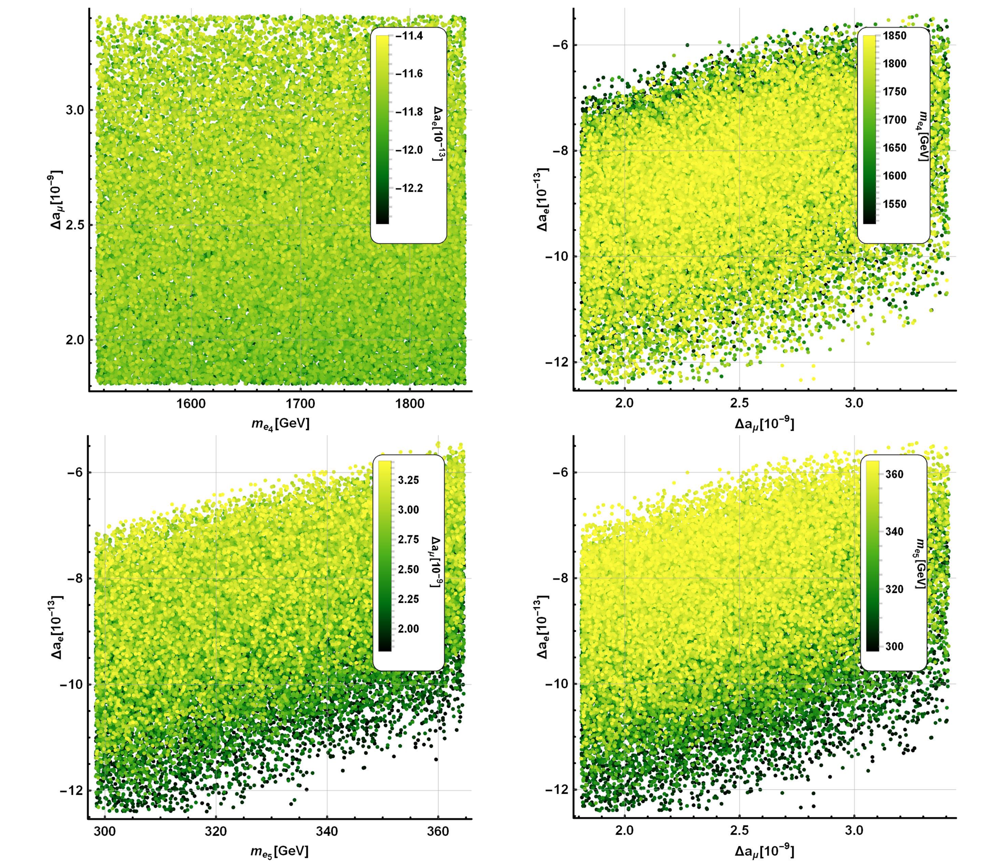

Figure 13: Available parameter spaces for the muon anomaly(electron anomaly) versus a relevant vector-like mass $m_{e_4}(m_{e_5})$

The total cross section for $pp \to H_1$ is given in Figure 14.

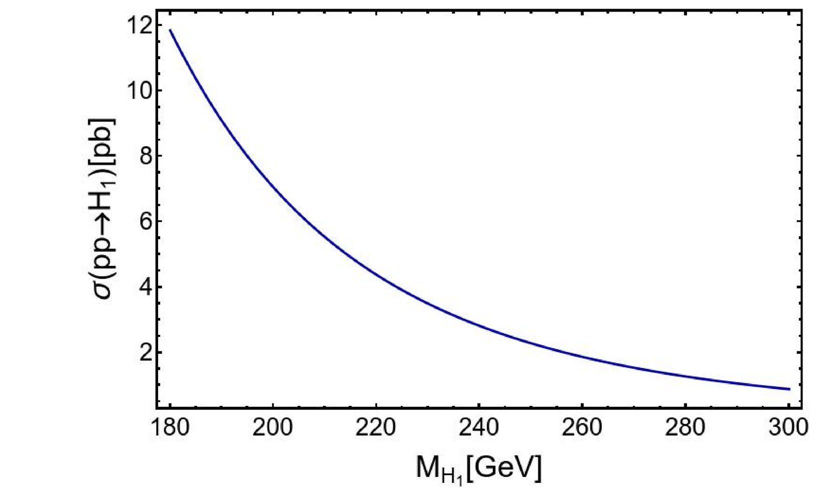

Figure 14: The total cross section for $pp \to H_1$ at $14\,\mathrm{TeV}$

The total cross section for $pp \to H_1$ runs from nearly $8\,\mathrm{pb}$ at $200\,\mathrm{GeV}$ to smaller values as mass of H_1 increases. The order of magnitude of this cross section for $pp \to H_1$ is compatible to that of the SM process $pp \to h$, however the BSM process is strongly suppressed since its single LHC production via gluon fusion mechanism is dominated by the triangular bottom quark loop. Therefore, our prediction with the light non-SM scalar H_1 is possible to accommodate each anomaly constraint at 1σ.

- S. F. King, JHEP **09**, 069 (2018) doi:10.1007/JHEP09(2018)069 [arXiv:1806.06780 [hep-ph]].
- L. Calibbi and G. Signorelli, Riv. Nuovo Cim. **41**, no. 2, 71 (2018) doi:10.1393/ncr/i2018-10144-0 [arXiv:1709.00294 [hep-ph]].
- E. Fernandez-Martinez, J. Hernandez-Garcia and J. Lopez-Pavon, JHEP **08**, 033 (2016) doi:10.1007/JHEP08(2016)033 [arXiv:1605.08774 [hep-ph]].
- M. Tanabashi *et al.* [Particle Data Group], Phys. Rev. D **98**, no.3, 030001 (2018) doi:10.1103/PhysRevD.98.030001
- J. Hernandez-Garcia and S. F. King, JHEP **05**, 169 (2019) doi:10.1007/JHEP05(2019)169 [arXiv:1903.01474 [hep-ph]].